Superconducting subphase in the layered perovskite ruthenate Sr_{2}RuO_{4} in a parallel magnetic field

Naoki Kikugawa, Taichi Terashima, Shinya Uji, Kaori Sugii, Yoshiteru Maeno, David Graf, Ryan Baumbach, and James Brooks

Phys. Rev. B **93**, 184513 — Published 31 May 2016

DOI: 10.1103/PhysRevB.93.184513

Superconducting Subphase in the Layered Perovskite Ruthenate Sr_2RuO_4 in Parallel Magnetic Field

Naoki Kikugawa and Taichi Terashima
National Institute for Materials Science, 3-13 Sakura, Tsukuba, Ibaraki 305-0003, Japan

Shinya Uji and Kaori Sugii*
National Institute for Materials Science, 3-13 Sakura, Tsukuba, Ibaraki 305-0003, Japan and Graduate School of Pure and Applied Sciences, University of Tsukuba, Tsukuba 305-8577, Japan

Yoshiteru Maeno
Department of Physics, Kyoto University, Kyoto 606-8502, Japan

David Graf, Ryan Baumbach, and James Brooks
National High Magnetic Field Laboratory, 1800 East Paul Dirac Drive, Tallahassee 32310, United States
(Dated: May 11, 2016)

Magnetic torque measurements using micro-cantilever have been performed to investigate the superconducting phase of Sr_2RuO_4 down to 40 mK. For high-quality single crystals with the transition temperature (T_c) of 1.48 – 1.49 K, an abrupt jump of the torque signal is found near 1.5 T in field parallel to the conducting RuO_2 planes below $\sim$0.8 K. The jump corresponds to the first order transition recently revealed by magnetocaloric and magnetization measurements [Yonezawa *et al.*, Phys. Rev. Lett. **110,** 077003 (2013); Kittaka *et al.*, Phys. Rev. B **90,** 220502(R) (2014)]. Furthermore, weak diamagnetic and irreversible signals are found to persist above the first order transition up to 1.85 T. The result indicates the presence of a subphase boundary separating low- and high-field phases in the superconducting phase. The high-field subphase disappears when the field is tilted from the conducting planes only by a few degrees. Quantum oscillation measurements are also reported to clarify the strong sample-quality dependence of the high-field subphase.

I. INTRODUCTION

Since the discovery of the superconductivity of the layered perovskite ruthenate Sr_2RuO_4 two decades ago [1], the material has attracted much attention because of novel superconductivity with the transition temperature (T_c) of 1.5 K [2, 3]. Some fascinating experimental results have been revealed. First, the fact that there is no change in the spin susceptibility across the T_c has been clarified by nuclear magnetic resonance (NMR) at different atomic sites [4–6] and polarized neutron scattering measurements [7]. Another is the presence of an internal magnetic field below T_c detected by muon spin relaxation measurement [8]. On the basis of these facts, it has been proposed that a spin-triplet pairing with broken time reversal symmetry is realized in the superconducting state [2, 3]. A recent measurement of tunneling spectra using a fabricated junction with Sr_2RuO_4 and Au [9] indicates a chiral edge state attributable to a chiral superconductivity. Thus, extensive studies on Sr_2RuO_4 have provided a new, topological aspect of superconductivity [3].

Despite these hallmarks of the novel superconductivity, a comprehensive understanding of the fundamental superconducting properties such as the temperature (T) dependence of the upper critical field (H_{c2}) is difficult to achieve. Reflecting the quasi two dimensional (2D) Fermi surfaces [10, 11], the H_{c2} is highly anisotropic, $\mu_0 H_{c2} = 1.5$ T (in-plane) and $= 0.075$ T (out-of-plane) for $H \parallel ab$ and $H \parallel c$, respectively [12]. Thermal conductivity [13], specific heat [14], ac susceptibility [15, 16], and magnetization [17] measurements suggest that H_{c2} for $H \parallel ab$ at low temperatures is suppressed; namely, it is much lower than expected from H_{c2} found for fields away from the in-plane direction. Those measurements present that the normal state abruptly recovers near $\mu_0 H_{c2} \sim 1.5$ T at low temperatures. This sudden recovery is remarkably weakened as the field direction is tilted from the conducting planes [13–16].

Recent experiments of the magnetocaloric effect using high quality samples demonstrate that the jump is thermodynamically attributed to a first order transition (FOT) for $T \leq 0.8$ K [18]. The observed FOT follows the $H_{c2} - T$ curves reported by other experiments [13–17]. The FOT is very sensitive to the field angle, and the transition changes to second order as the field is tilted from the RuO_2 planes [18]. The FOT was also observed by recent magnetization and magnetic torque measurements using a capacitive Faraday magnetometer [19]. However, the origin of the FOT and the strong field angle dependence, which are expected to be closely related to the superconducting symmetry, still remain unclear.

We have performed magnetic torque (τ) measurements using a micro-cantilever, which is a highly sensitive probe to detect bulk superconducting diamagnetism [20], in order to deepen our understanding of the superconducting

* Present address: The Institute for Solid State Physics, The University of Tokyo, Kashiwa, Chiba 277-8581, Japan

properties of Sr_2RuO_4. For high quality samples with $T_c = 1.48$, and 1.49 K, we observe a clear superconducting diamagnetic response associated with hysteresis even above the FOT field (1.5 T) in field parallel to the RuO_2 planes, suggesting the presence of a high-field subphase. We also find the characteristic field-angle and temperature dependences of the superconducting phases with different sample qualities.

II. EXPERIMENTAL

Single crystals of Sr_2RuO_4 were grown by a floating-zone method. Temperature dependence of the interlayer resistance without field shows no sign of the inclusion of the so-called "3-K phase" in Ru-Sr_2RuO_4 eutectic system [21]. For the magnetic torque measurements, the boule was cut into small pieces with the typical size of 0.20 mm × 0.25 mm × 0.03 mm in [100], [010] and [001] directions, respectively. Here, the sample size used in this study was much smaller than that used for the previous magnetocaloric effect [18], magnetization, and magnetic torque measurements [19]. The onset T_c of the crystals labeled as ♯1, ♯2, and ♯3 were 1.49, 1.48 and 1.44 K, respectively. All the experiments under magnetic fields were performed by using dilution fridges mounted in superconducting magnets at NIMS and NHMFL. The field angle (θ) is measured from [100] (or [110] for part of data in Figs. 4(a) and (d)) to [001], as shown in the inset of Fig. 2(b). For simplicity, we hereafter represent measurements at 0.3° off the exact [100] and [110] directions as $H \parallel [100]$ and $H \parallel [110]$, respectively. Since the magnetic torque diminishes at symmetry directions, such tilting is necessary to gain the sufficient torque signal.

III. RESULTS AND DISCUSSION

Figure 1(a) shows the field dependence of the magnetic torque (τ) at 40 mK under $H \parallel [100]$. The magnetization curve given by $\tau/(\mu_0 H)$ for ♯1 is presented in the inset of Fig. 1(a). The result is very similar to that seen by means of a capacitive Faraday force method, including a kink around 0.9 T [17] (denoted as H_k in Ref. [17]). The overall behavior of the torque curves, associated with hysteresis, seems similar for all the samples but a significant difference is evident at ∼1.5 T. A jump, indicating a FOT, is seen for samples ♯1 and ♯2 but a rather continuous change for ♯3. The transition at 1.5 T is very sensitive to the sample quality, as already noted in Ref. [18].

Figure 1(b) presents the close-up views of the torque signals near 1.6 T. Interestingly, the diamagnetic signal is observed beyond 1.5 T, which is the most evident for ♯1 with $T_c = 1.49$ K. The diamagnetism disappears at 1.85 T for ♯1. At the same field, the torque curves become reversible. In order to deduce the irreversible field H_{irr}, we introduce $\Delta\tau$ that represents the difference of the torque signals between up- and down-field sweeps, as examined in Ref. [22]. In Fig. 1(c), field dependence of $\Delta\tau$ was shown. Here, the H_{irr} is indicated by a thick arrow. Similar irreversible behavior is seen for ♯2, but the diamagnetism and hysteresis above 1.5 T are much smaller. Finally, for ♯3 with $T_c = 1.44$ K, neither FOT behavior nor small diamagnetism above 1.5 T was seen. H_{irr} above $T \sim 0.8$ K coincides with bulk H_{c2} as explained below, which excludes the possibilities that the diamagnetic signal above 1.5 T is due to the so-called "3-K phase" in Ru-Sr_2RuO_4 eutectic system [3, 21] or surface superconductivity. Small diamagnetism has been observed above H_{c2} in highly anisotropic superconductors such as organic compounds [23, 24] and it is ascribed to superconducting fluctuation. However, the present diamagnetism above 1.5 T for these samples cannot be ascribed to superconducting fluctuation since the strong vortex pinning suggested by the irreversibility is not expected in the fluctuation regime [23, 24]. We conclude that the bulk phase coherence of the superconductivity is preserved at least up to H_{irr}.

We present the torque curves at various temperatures in Figs. 2(a) and (c), and the curves at various field angles in Figs. 2(b) and (d) for ♯1. Again, the $\Delta\tau$ curves (Figs. 2(c) and (d)) are the differences of the torque signals between up- and down-field-sweeps, where the H_{irr} is well defined as shown by arrows. The diamagnetic torque signal is suppressed and H_{irr} is reduced with increasing temperature. In addition, the torque signal jump becomes less obvious with increasing temperature. In Fig 2(d), the H_{irr} is also reduced as the field is tilted from the plane. The jump is not evident above ∼2 degrees (Fig. 2(b)), consistent with the result of the magnetocaloric effect [18]. For comparison, we present torque curves for ♯3 at various temperatures (Figs. 3(a) and (c)) and at various field angles (Figs. 3(b) and (d)) in order to deduce the H_{irr} for this sample. It is obvious that the jumps are not observed at any temperature or angle. That is in sharp contrast to the behavior seen in ♯1.

We summarize our results in field (H)–temperature (T) phase-diagrams in Figs 4(a), (b) and (c) for ♯1, ♯2, and ♯3, respectively. In Fig. 4(c), H_{c2} obtained from ac susceptibility measurements [16] is also plotted, which agrees well with H_{irr} in sample ♯3 and also with H_{irr} in samples ♯1 and ♯2 for $T \geq 0.8$ K. H_{irr} for ♯3 agrees well with H_{c2} from other ac susceptibility [15, 25], thermal conductivity [13] and specific heat measurements [14]. Significant features are seen in the low temperature and high-field region; H_{irr} is well beyond 1.5 T for ♯1 and ♯2. It seems that, if extrapolated, the FOT field (H_{1st}) line is smoothly connected to the H_{irr} line at ∼0.8 K, and ∼1.2 T, although it is difficult to identify the FOT field (H_{1st}) above 0.7 K. The H_{irr} values for ♯1 with $T_c = 1.49$ K are apparently higher than those for ♯2 with $T_c = 1.48$ K. We stress that H_{irr} is directly deduced, not extrapolated [13, 14], on the basis of the simple definition of the irreversible field on type II superconductivity. A similar phase diagram is obtained when the field is

applied along [110] for ♯1 [open symbols in Fig. 4(a)].

The angular dependence studies are summarized in Figs. 4(d), (e), and (f) for ♯1, ♯2, and ♯3, respectively. At $T = 40\,\mathrm{mK}$, $H_{1\mathrm{st}}$ of ♯1 and ♯2 is reduced with increasing angle and seems to smoothly merge with H_{irr} at $\theta \sim 3^\circ$ if the angular dependence is extrapolated. On the other hand, H_{irr} of ♯3 is not enhanced but identical to $H_{1\mathrm{st}}$ of ♯1 and ♯2 at $\theta \leq 3^\circ$, which corresponds to "H_{c2} suppression" reported in previous studies [13–18]. Interestingly, taking $\Gamma = 26$ and $\mu_0 H_{\mathrm{irr0}} = 1.85\,\mathrm{T}$, we can fit the $H_{\mathrm{irr}}(\theta)$ data at 40 mK with a conventional anisotropic effective mass model, $H_{\mathrm{irr}}(\theta) = \frac{H_{\mathrm{irr0}}}{\sqrt{\cos^2\theta + \Gamma^2 \sin^2\theta}}$, in the entire angle range ($0^\circ \leq \theta \leq 90^\circ$) for ♯1, as shown by the top solid curve (green) in Fig. 4(d). The same parameters cannot reproduce the $H_{\mathrm{irr}}(\theta)$ data at low angles for the other samples, as shown by the top solid curves (green) in Figs. 4(e) and (f). In contrast, $H_{\mathrm{irr}}(\theta)$ at $T \sim 0.9\,\mathrm{K}$ is almost similar for all three samples, which can be fitted with the same parameters ($\Gamma = 26$ and $H_{\mathrm{irr0}} = 1.15\,\mathrm{T}$), as presented by the middle solid curves (purple) in Figs. 4(d)-(f). Note that the H_{c2} anisotropy $\Gamma = 26$ obtained above differs from the coherence length anisotropy $\Gamma \sim 60$ estimated at low fields ($0.5 \sim 0.7\,\mathrm{T}$) from small-angle neutron scattering (SANS) experiments [26] and the angular dependence of magnetic torque [19].

The irreversible feature and H_{irr} value strongly depend on T_{c} of the sample, which is probably related to the sample quality. It is known that T_{c} of Sr_2RuO_4 is extremely sensitive to any kinds of disorder or impurities [27–29]. Recently, it is reported that the T_{c} can be also be controlled by external strain [30, 31]. However, the strain effect on T_{c} can be excluded in this study, because samples were not under strain during the experiments. In order to check the sample quality in more detail, we performed quantum oscillation measurements of all the samples at 40 mK by applying the field almost perpendicular to the RuO_2 plane up to 17.5 T. Here, we used the same experimental setup as used above to determine the phase diagrams, and the deviation between the field and the c axis was 3.0, 3.2, and 4.5 degrees for ♯1, ♯2, and ♯3, respectively. Figure 5(a) shows the de Haas-van Alphen oscillations in a low field region. Clear oscillations attributed to the α branch [10, 32] are observed above 2 T for ♯1 and ♯2, but above $\sim 2.4\,\mathrm{T}$ for ♯3 [Fig. 5(a)]. The slope of the Dingle plot in Fig. 5(b), (c), and (d) gives the Dingle temperature (T_{D}) for the α, β, and γ branch, respectively. For instance, the T_{D} for α branch was obtained as 0.20, 0.19 and 0.28 K for ♯1, ♯2, and ♯3, respectively. Then, we can evaluate the mean free path (ℓ_i) for each branch ($i = \alpha$, β, and γ), using the relations $T_{\mathrm{D}i} = \hbar/(2\pi k_{\mathrm{B}} \tau_i)$ and $\ell_i = v_{\mathrm{F}i}\tau_i$ [33]. Here, $\hbar$ is the Plank constant, k_{B} the Boltzmann constant, $v_{\mathrm{F}i}$ the Fermi velocity, and τ_i the scattering time. Figure 5(e) presents the ℓ_i vs. H_{irr} plot for all the samples. It is clear that higher T_{c} values correlate with longer mean-free-path as expected for the unconventional superconductivity of Sr_2RuO_4. Since the in-plane superconducting coherence length ($\xi_{ab} \sim 66\,\mathrm{nm}$) [12] is much shorter than ℓ_i, the superconductivity for all the samples is in a clean limit. The important fact is that the long mean free path (high quality) is required for the FOT and large H_{irr}.

Here, we consider the origin of the FOT, the subphase boundary ($H_{1\mathrm{st}}$) in the superconducting phase. Recent NMR measurements have suggested an equal-spin pairing state with a chiral p-wave superconducting state [34]. In the simple triplet scenario, a modification of the d-vector would be possible reflecting the internal degrees of freedom for both spin part and orbital part, because the candidate d-vectors in a tetragonal symmetry are found to be almost degenerate [35]. A crossover to a non-unitary state in a low-temperature and high-field region has been proposed theoretically in the case that a weak spin-orbit coupling is taken into account [36]. Although the transformation to the non-unitary state is a crossover, not a FOT, it would be interesting if a small superconducting signal above $H_{1\mathrm{st}}$ reflects the non-unitary state, where only one spin direction is paired, indicating the other spin direction has a zero gap.

Another aspect to be considered is that the simple triplet formula may break down because of the entanglement between orbitals and spin through a strong spin-orbit coupling ($\sim 0.2\,\mathrm{eV}$) experimentally revealed by spin- and orbital-resolved photoemission spectroscopy [37] and by resonant inelastic x-ray scattering measurement [38]. The entanglement is significant for β and γ bands, while such an effect is insignificant for α band [37]. Samples ♯1 and ♯2, which have longer mean free paths for β and γ than ♯3, have enhanced H_{irr}. This may indicate that long scattering time is necessary for the entanglement not to be destroyed by scattering. The entanglement could yield a novel superconductivity with both singlet- and triplet-paring [39]. In that case, a paramagnetic effect is no longer negligible. The observed subphase above $H_{1\mathrm{st}}$ emerges only under the following conditions: (1) high quality samples satisfying the highly clean limit regime ($\ell_i \gg \xi_{ab}$), (2) low temperature and high field, (3) well-aligned field angle to the conducting planes where the orbital effect is quenched ($\theta \leq 3^\circ$). These conditions remind us of a FOT caused by a paramagnetic effect [40–43] and/or spatially modulated superconductivity proposed by Flude-Ferrel and Larkin-Ovchinnikov (FFLO) [44–46]. Here the clear evidence for the FFLO state has recently been reported in organic compounds [47–49] and a heavy fermion system $CeCoIn_5$ [50–52]. Theoretical calculations taking the paramagnetic effect into account have been proposed to explain experimental aspects such as field dependence of the specific heat, and H_{c2} suppression in Sr_2RuO_4 [41, 53–55]. The consideration of the mixture of both singlet- and triplet-pairing would be promising for fully understanding of the novel superconductivity in Sr_2RuO_4.

IV. SUMMARY

We presented the significant purity dependence of the superconducting phase diagram of Sr_2RuO_4 at low temperatures when the field is well aligned to the conducting planes. For the purest sample with $T_c = 1.49\,\mathrm{K}$, we have experimentally found that the small but clear diamagnetic signals persisting up to $H_{irr} = 1.85\,\mathrm{T}$ beyond the FOT field $\sim 1.5\,\mathrm{T}$ for the first time. This indicates that a high-field superconducting subphase exists above the FOT. We are able to fit the angular dependence of H_{irr} in the entire angle range using a conventional anisotropic mass model as if the "H_{c2} suppression" is relieved. We have also presented the relation between the existence of the high-field subphase and quasiparticle lifetime through the quantum oscillation measurements.

V. ACKNOWLEDGEMENTS

We acknowledge S. Yonezawa, K. Ishida, H. Yaguchi, and Y. Yanase for useful discussion. This work is partly supported by Grants-in-Aid for Scientific Research (KAKENHI Grants Nos. 22103002, 25400384 and 15H05852) from MEXT. N.K. acknowledges the support of overseas researcher dispatch program in NIMS. Also, a portion of this work was performed at the National High Magnetic Field Laboratory, which is supported by National Science Foundation (NSF) Cooperative Agreement No. DMR-1157490, the State of Florida, and the U.S. Department of Energy (DOE NNSA DE-NA0001979). J.B. acknowledges the support from NSF-DMR-1309146.

[1] Y. Maeno, H. Hashimoto, K. Yoshida, S. Nishizaki, T. Fujita, J. G. Bednorz, and F. Lichtenberg, Nature **372**, 532 (1994).
[2] A. P. Mackenzie and Y. Maeno, Rev. Mod. Phys. **75**, 657 (2003).
[3] Y. Maeno, S. Kittaka, T. Nomura, S. Yonezawa, and K. Ishida, J. Phys. Soc. Jpn. **81**, 11009 (2012).
[4] K. Ishida, H. Mukuda, Y. Kitaoka, K. Asayama, Z. Mao, Y. Mori, and Y. Maeno, Nature **396**, 658 (1998).
[5] K. Ishida, H. Mukuda, Y. Kitaoka, Z. Mao, Y. Mori, and Y. Maeno, Phys. Rev. Lett. **84**, 5387 (2000).
[6] H. Murakawa, K. Ishida, K. Kitagawa, Z. Mao, and Y. Maeno, Phys. Rev. Lett. **93**, 167004 (2004).
[7] J. Duffy, S. Hayden, Y. Maeno, Z. Mao, J. Kulda, and G. McIntyre, Phys. Rev. Lett. **85**, 5412 (2000).
[8] G. Luke, Y. Fudamoto, K. Kojima, M. Larkin, J. Merrin, B. Nachiumi, Y. J. Uemura, Y. Maeno, Z. Mao, Y. Mori, H. Nakamura, and M. Sigrist, Nature **394**, 558 (1998).
[9] S. Kashiwaya, H. Kashiwaya, H. Kambara, T. Furuta, H. Yaguchi, Y. Tanaka, and Y. Maeno, Phys. Rev. Lett. **107**, 077003 (2011).
[10] A. P. Mackenzie, S. R. Julian, A. J. Diver, G. J. McMullan, M. P. Ray, G. G. Lonzarich, Y. Maeno, S. Nishizaki, and T. Fujita, Phys. Rev. Lett. **76**, 3786 (1996).
[11] A. Damascelli, D. Lu, K. Shen, N. Armitage, F. Ronning, D. Feng, C. Kim, Z.-X. Shen, T. Kimura, Y. Tokura, Z. Mao, and Y. Maeno, Phys. Rev. Lett. **85**, 5194 (2000).
[12] T. Akima, S. NishiZaki, and Y. Maeno, J. Phys. Soc. Jpn. **68**, 694 (1999).
[13] M. Tanatar, S. Nagai, Z. Mao, Y. Maeno, and T. Ishiguro, Phys. Rev. B **63**, 064505 (2001).
[14] K. Deguchi, M. A. Tanatar, Z. Mao, T. Ishiguro, and Y. Maeno, J. Phys. Soc. Jpn. **71**, 2839 (2002).
[15] H. Yaguchi, T. Akima, Z. Mao, Y. Maeno, and T. Ishiguro, Phys. Rev. B **66**, 214514 (2002).
[16] S. Kittaka, T. Nakamura, Y. Aono, S. Yonezawa, K. Ishida, and Y. Maeno, Phys. Rev. B **80**, 174514 (2009).
[17] K. Tenya, S. Yasuda, M. Yokoyama, H. Amitsuka, K. Deguchi, and Y. Maeno, J. Phys. Soc. Jpn. **75**, 23702 (2006).
[18] S. Yonezawa, T. Kajikawa, and Y. Maeno, Phys. Rev. Lett. **110**, 77003 (2013).
[19] S. Kittaka, A. Kasahara, T. Sakakibara, D. Shibata, S. Yonezawa, Y. Maeno, K. Tenya, and K. Machida, Phys. Rev. B **90**, 220502 (2014).
[20] C. Rossel, P. Bauer, D. Zech, J. Hofer, M. Willemin, and H. Keller, J. Appl. Phys. **79**, 8166 (1996).
[21] T. Ando, T. Akima, Y. Mori, and Y. Maeno, J. Phys. Soc. Jpn. **68**, 1651 (1999).
[22] N. Kurita, K. Kitagawa, K. Matsubayashi, A. Kismarahardja, E.-S. Choi, J. S. Brooks, Y. Uwatoko, S. Uji, and T. Terashima, J. Phys. Soc. Jpn. **80**, 13706 (2011).
[23] S. Tsuchiya, J. Yamada, S. Tanda, K. Ichimura, T. Terashima, N. Kurita, K. Kodama, and S. Uji, Phys. Rev. B **85**, 220506 (2012).
[24] S. Tsuchiya, J.-i. Yamada, K. Sugii, D. Graf, J. S. Brooks, T. Terashima, and S. Uji, J. Phys. Soc. Jpn. **84**, 034703 (2015).
[25] Z. Mao, Y. Maeno, S. NishiZaki, T. Akima, and T. Ishiguro, Phys. Rev. Lett. **84**, 991 (2000).
[26] C. Rastovski, C. D. Dewhurst, W. J. Gannon, D. C. Peets, H. Takatsu, Y. Maeno, M. Ichioka, K. Machida, and M. R. Eskildsen, Phys. Rev. Lett. **111**, 087003 (2013).
[27] A. Mackenzie, R. Haselwimmer, A. Tyler, G. Lonzarich, Y. Mori, S. Nishizaki, and Y. Maeno, Phys. Rev. Lett. **80**, 161 (1998).
[28] Z. Mao, Y. Mori, and Y. Maeno, Phys. Rev. B **60**, 610 (1999).
[29] N. Kikugawa, A. P. Mackenzie, and Y. Maeno, J. Phys. Soc. Jpn. **72**, 237 (2003).
[30] S. Kittaka, H. Taniguchi, S. Yonezawa, H. Yaguchi, and Y. Maeno, Phys. Rev. B **81**, 180510 (2010).
[31] C. W. Hicks, D. O. Brodsky, E. A. Yelland, A. S. Gibbs, J. A. N. Bruin, M. E. Barber, S. D. Edkins, K. Nishimura, S. Yonezawa, Y. Maeno, and A. P. Mackenzie, Science **344**, 283 (2014).
[32] C. Bergemann, a. P. Mackenzie, S. R. Julian, D. Forsythe, and E. Ohmichi, Adv. Phys. **52**, 639 (2003).
[33] D. Shoenberg, *Magnetic Oscillations in Metals* (Cambridge University Press, 1984).

[34] K. Ishida, M. Manago, T. Yamanaka, H. Fukazawa, Z. Q. Mao, Y. Maeno, and K. Miyake, Phys. Rev. B **92**, 100502 (2015).
[35] Y. Yanase and M. Ogata, J. Phys. Soc. Jpn. **72**, 673 (2003).
[36] M. Udagawa, Y. Yanase, and M. Ogata, J. Phys. Soc. Jpn. **74**, 2905 (2005).
[37] C. N. Veenstra, Z.-H. Zhu, M. Raichle, B. M. Ludbrook, A. Nicolaou, B. Slomski, G. Landolt, S. Kittaka, Y. Maeno, J. H. Dil, I. S. Elfimov, M. W. Haverkort, and A. Damascelli, Phys. Rev. Lett. **112**, 127002 (2014).
[38] C. G. Fatuzzo, M. Dantz, S. Fatale, P. Olalde-Velasco, N. E. Shaik, B. Dalla Piazza, S. Toth, J. Pelliciari, R. Fittipaldi, A. Vecchione, N. Kikugawa, J. S. Brooks, H. M. Rønnow, M. Grioni, C. Rüegg, T. Schmitt, and J. Chang, Phys. Rev. B **91**, 155104 (2015).
[39] M. Haverkort, I. Elfimov, L. Tjeng, G. Sawatzky, and A. Damascelli, Phys. Rev. Lett. **101**, 026406 (2008).
[40] K. Maki, Phys. Rev. **148**, 362 (1966).
[41] K. Machida and M. Ichioka, Phys. Rev. B **77**, 184515 (2008).
[42] T. Terashima, K. Kihou, M. Tomita, S. Tsuchiya, N. Kikugawa, S. Ishida, C.-H. Lee, A. Iyo, H. Eisaki, and S. Uji, Phys. Rev. B **87**, 184513 (2013).
[43] D. A. Zocco, K. Grube, F. Eilers, T. Wolf, and H. v. Löhneysen, Phys. Rev. Lett. **111**, 057007 (2013).
[44] P. Fulde and R. A. Ferrell, Phys. Rev. **135**, A550 (1964).
[45] A. Larkin and Y. Obchinnikov, Sov. Phys. JETP **20**, 762 (1965).
[46] Y. Matsuda and H. Shimahara, J. Phys. Soc. Jpn. **76**, 51005 (2007).
[47] S. Uji, T. Terashima, M. Nishimura, Y. Takahide, T. Konoike, K. Enomoto, H. Cui, H. Kobayashi, A. Kobayashi, H. Tanaka, M. Tokumoto, E. Choi, T. Tokumoto, D. Graf, and J. Brooks, Phys. Rev. Lett. **97**, 157001 (2006).
[48] R. Lortz, Y. Wang, A. Demuer, P. Böttger, B. Bergk, G. Zwicknagl, Y. Nakazawa, and J. Wosnitza, Phys. Rev. Lett. **99**, 187002 (2007).
[49] S. Uji, K. Kodama, K. Sugii, T. Terashima, Y. Takahide, N. Kurita, S. Tsuchiya, M. Kimata, A. Kobayashi, B. Zhou, and H. Kobayashi, Phys. Rev. B **85**, 1 (2012).
[50] A. Bianchi, R. Movshovich, C. Capan, P. G. Pagliuso, and J. L. Sarrao, Phys. Rev. Lett. **91**, 187004 (2003).
[51] C. F. Miclea, M. Nicklas, D. Parker, K. Maki, J. L. Sarrao, J. D. Thompson, G. Sparn, and F. Steglich, Phys. Rev. Lett. **96**, 117001 (2006).
[52] V. Correa, T. Murphy, C. Martin, K. Purcell, E. Palm, G. Schmiedeshoff, J. Cooley, and S. Tozer, Phys. Rev. Lett. **98**, 087001 (2007).
[53] A. G. Lebed and N. Hayashi, Phys. C Supercond. **341-348**, 1677 (2000).
[54] Y. Amano, M. Ishihara, M. Ichioka, N. Nakai, and K. Machida, Phys. Rev. B **91**, 144513 (2015).
[55] N. Nakai and K. Machida, Phys. Rev. B **92**, 054505 (2015).

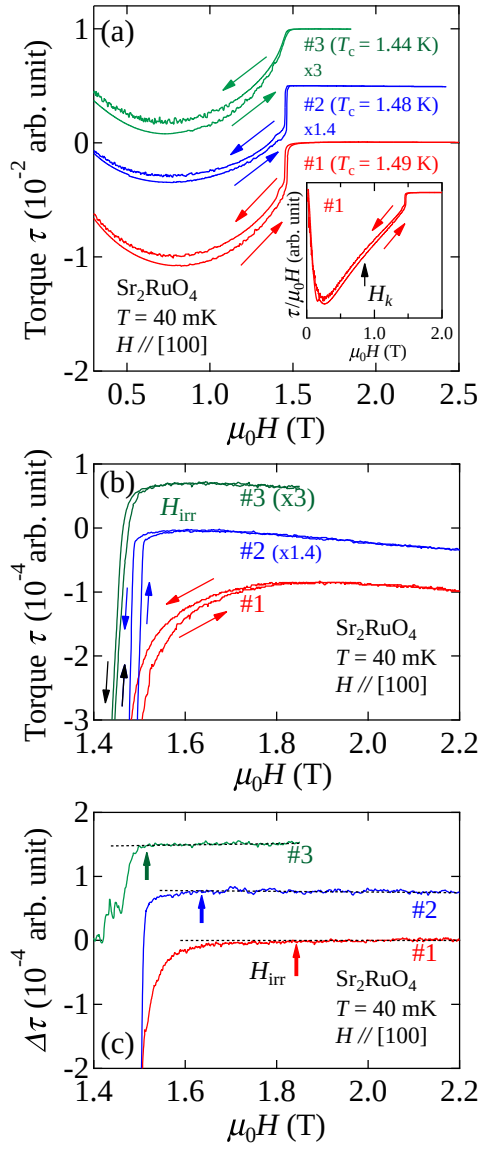

FIG. 1. (color online) (a) Field dependence of the magnetic torque (τ) for samples ♯1, ♯2, and ♯3 under $H \parallel [100]$ at $T = 40$ mK. The arrows show the field-up and -down sweep. The inset shows the field dependence of the magnetization obtained by $\tau/(\mu_0 H)$ for ♯1. (b) Magnetic field dependence of the torque around 1.6 T. (c) Field dependence of $\Delta\tau$, difference in τ between up- and down-field-sweeps. The thick vertical arrows indicate H_{irr}. Although labeled $H \parallel [100]$, the field was applied 0.3° off [100] to observe sufficient torque signals. Data are offset for clarity.

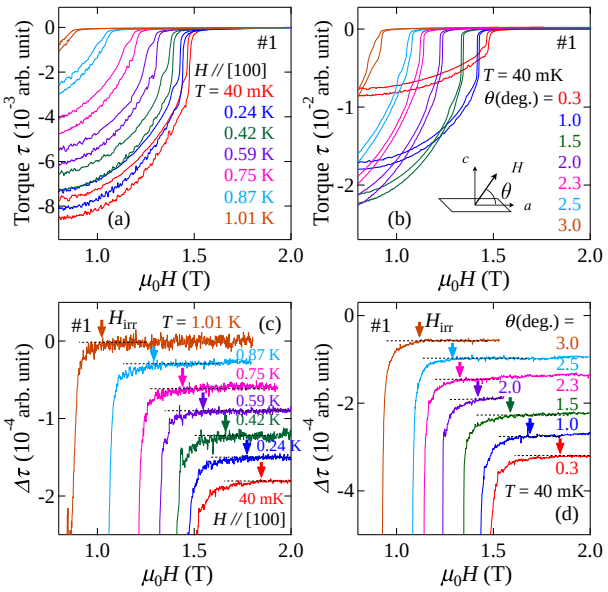

FIG. 2. (color online) (a) Field dependence of the magnetic torque (τ) under several temperatures at $H \parallel [100]$ for sample ♯1. (b) Field dependence of the magnetic torque for ♯1 under the various field angles at 40 mK. The inset shows the definition of the angle θ from [100] to [001]. (c) Field dependence of $\Delta\tau$, difference in τ between up- and down-field-sweeps, to deduce $H_{\rm irr}(T)$ for ♯1. The thick arrows present the $H_{\rm irr}$. The curves are offset for clarity. (d) Field dependence of $\Delta\tau$ under various angle θ to deduce the $H_{\rm irr}(\theta)$ for ♯1. The thick arrows represent $H_{\rm irr}$. The curves are offset for clarify. Note that although labeled $H \parallel [100]$, the data in (a) and (c) were obtained with the field 0.3° off [100]. Data are offset for clarity.

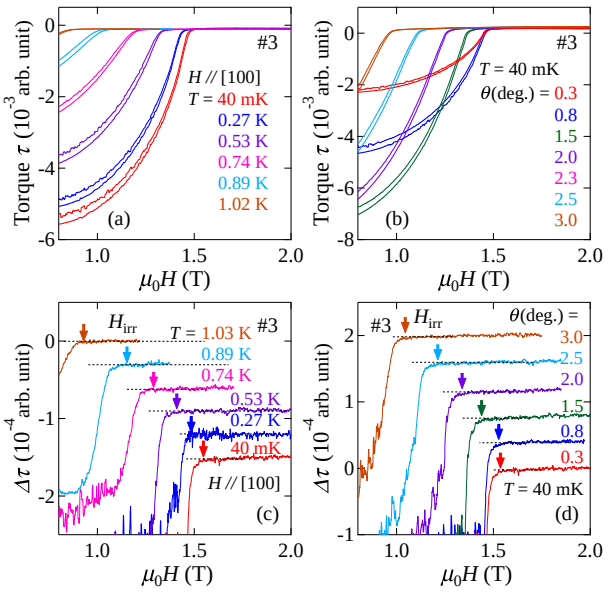

FIG. 3. (color online) (a) Field dependence of the magnetic torque τ under several temperatures at $H \parallel [100]$ for sample ♯3. (b) Field dependence of the magnetic torque for ♯3 under the various field angles at 40 mK. (c,d) Field dependence of $\Delta\tau$ to deduce $H_{\rm irr}(T)$ and $H_{\rm irr}(\theta)$ for ♯3. The thick arrows present the $H_{\rm irr}$. The curves are offset for clarity. Note that although labeled $H \parallel [100]$, the data in (a) and (c) were obtained with the field 0.3° off [100]. Data are offset for clarity.

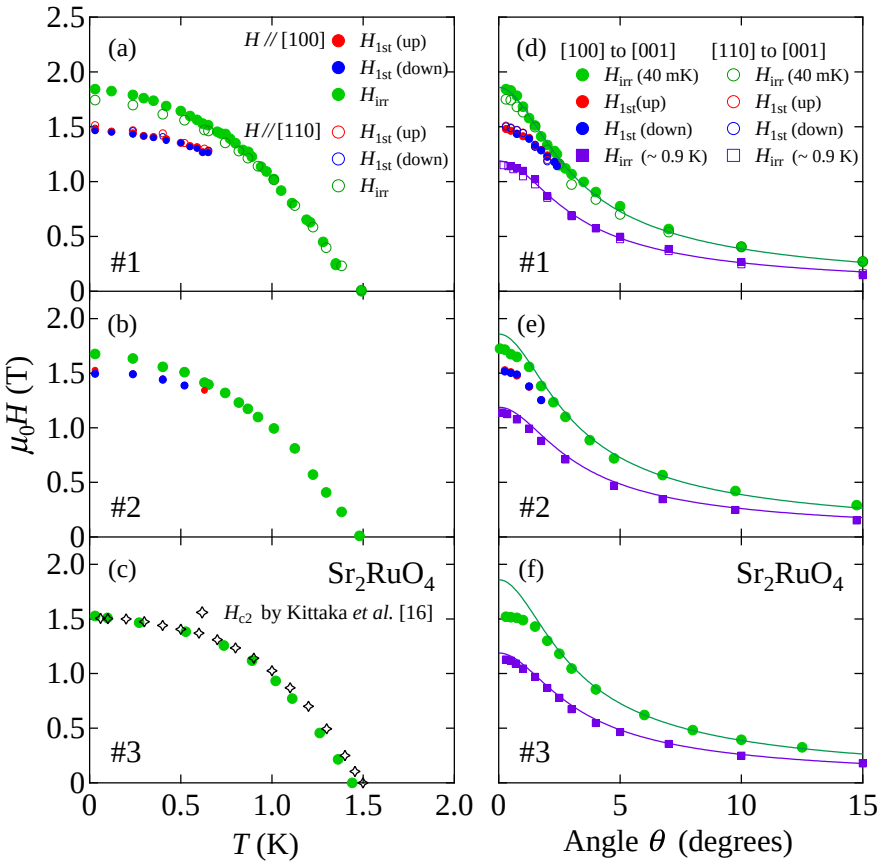

FIG. 4. (color online) (a,b,c) Field-temperature phase diagram of Sr_2RuO_4 for (a) sample ♯1, (b) ♯2, and (c) ♯3 under $H \parallel [100]$. For sample ♯1, we also show the results under $H \parallel [110]$ with open symbols. Although labeled $H \parallel [100]$ ($\parallel [110]$), the field was applied 0.3° off from the exact [100] ($\parallel [110]$) in order to gain sufficient torque signals. H_{c2} data from Ref. [16] is added in (c) for comparison. (d,e,f) Field-angle phase diagram of Sr_2RuO_4 for (d) sample ♯1, (e) ♯2, and (f) ♯3 at $T = 40$ mK and ~ 0.9 K. For sample ♯1, we also show the results for fields tilted from $H \parallel [110]$ with open symbols. The top solid curve (green) for (d) shows the $H_{irr}(\theta)$ fitting at $T = 40$ mK using a conventional anisotropic effective mass model, while the second solid curve (purple) at $T = 0.9$ K. Using the same parameters for sample ♯1, we plot the curves for ♯2, and ♯3 in (e) and (f), respectively.

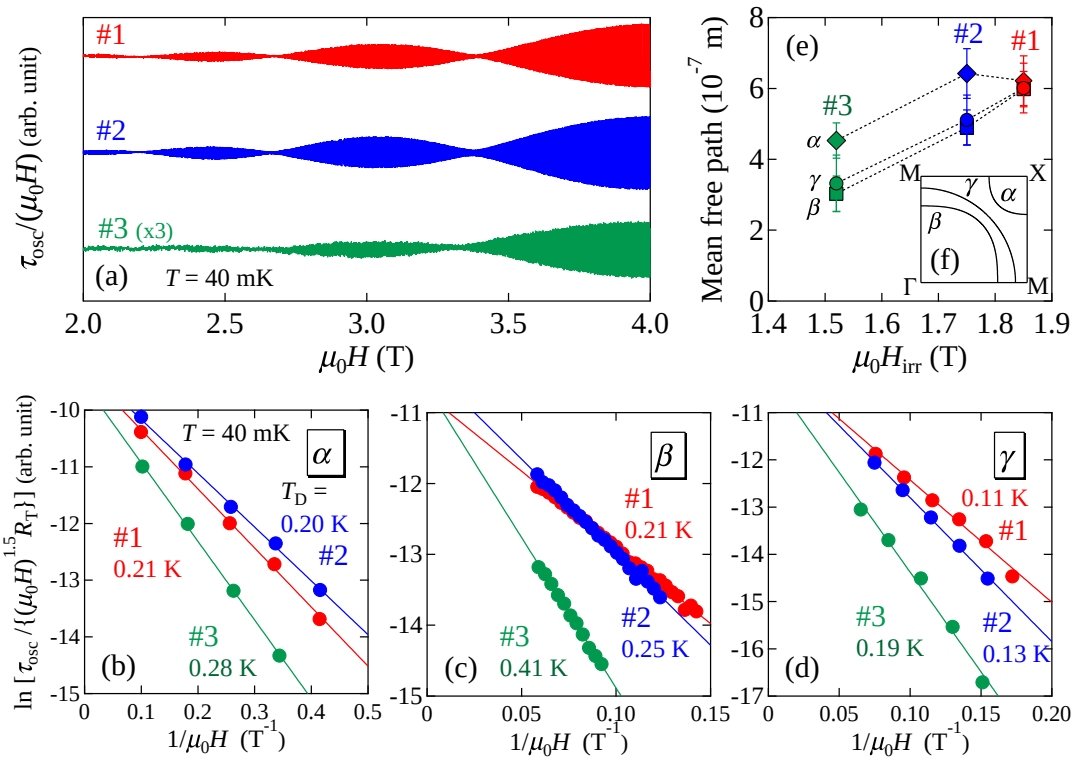

FIG. 5. (color online) (a) Quantum oscillations originating from α band for all the samples. The field was applied 3.0, 3.2, and 4.5 degree off the c axis for ♯1, ♯2, and ♯3, respectively. (b,c,d) Dingle plots of the α, β, and γ branch are shown in (b), (c), (d), respectively. The solid lines are fits to deduce the Dingle temperatures $T_{\rm D}$. (e) Relation between the mean free paths ℓ_i for the three bands of Sr_2RuO_4 ($i = \alpha$, β, and γ) and the irreversible fields $H_{\rm irr}$ for all the samples in this study. (f) A sketch of the electronic structure of Sr_2RuO_4.